Materials Advances

ROYAL SOCIETY OF CHEMISTRY

PAPER

View Article Online
View Journal | View Issue

Cite this: *Mater. Adv.*, 2023, 4, 2301

Aldol condensation-polymerized semiconducting polymers based on a BDOPV unit with near infrared absorption and better n-doped ability†

Li Tian, *[a] Airong Wang,[b] Haowei Lin,[a] Wenxi Cheng,[a] Mengya Shang,[a] Shanhong Xu[a] and Xuefei Zhou[a]

Received 16th February 2023,
Accepted 11th April 2023

DOI: 10.1039/d3ma00073g

rsc.li/materials-advances

Development of semiconducting polymers with a low bandgap is essential for organic electronic devices. However, most of the currently reported organic semiconductors possess absorption edges of less than 1000 nm. Herein, a series of novel semiconducting polymers with a low bandgap and better n-doping behavior were synthesized. These semiconducting polymers based on a benzodifurandione-centered oligo(*p*-phenylene vinylene) (BDOPV) unit and various copolymerization units were synthesized *via* a modified aldol condensation protocol from bis-isatin and bis-oxindole monomers. As a result, the polymers with different constitutional units present various charge transfer characteristics, from the n-type character for PFBP switched into an ambipolar and even p-type character for PBBP. In addition, these semiconducting polymers can be easily doped with an n-type dopant, such as *N*-DMBI. We believe that this BDOPV-based polymer is a potential candidate for the development of low bandgap semiconducting polymers.

1. Introduction

Semiconducting polymers with flexibility, abundance of sources, outstanding solution processability and adjustable optoelectric properties have tremendous applications in organic photoelectric devices, such as organic photodetectors,[1,2] organic light emitting diodes,[3,4] and organic solar cells.[5–7] Moreover, due to their excellent mechanical properties and superb thermo-mechanical stability over small molecule semiconductors, semiconducting polymers exhibit huge application prospects in the fabrication of flexible and stretchable electronics. Over the past few decades, a number of new semiconducting polymers with a variety of photoelectric properties have been designed and synthesized.[8–13]

In solar radiation energy, near-infrared (NIR) light ($780 < \lambda < 2500$ nm) accounts for about 52% of solar photons.[14] Narrow-bandgap semiconducting polymers with a red-shift absorbing edge can harvest many more photons in the near infrared region and improve the utilization of solar energy.[15] Through optimization of a conjugated structure, a number of narrow-bandgap small molecule semiconductors have been reported.[16–19] However, compared to semiconducting small molecules, semiconducting polymers based on an NDI unit (*e.g.* N2200) always have a wide bandgap.[20–23] Therefore, it is of great significance to develop novel semiconducting polymers with new conjugated backbones to further narrow the bandgap. In addition to the rational design of novel semiconducting polymers, the doping effect can also efficiently tune the properties of semiconducting polymers, and broaden the absorption spectrum.[24–26] Due to their easy synthesis, convenient device processing, and potential for solution preparation, the introduction of additional dopants into conjugated backbones is a promising method to realize efficient absorption in the near infrared region.[27–29]

Benzodifurandione-centered oligo(*p*-phenylene vinylene) (BDOPV) is a class of ideal building blocks for narrow-bandgap semiconducting polymers. Semiconducting polymers with BDOPV usually have a low-lying LUMO and a planar conjugated backbone which is in favor of intramolecular charge transfer (ICT) and doping behavior.[24] However, due to the unstable ester group in the BDOPV unit, a disruptive ring opening reaction could occur during Suzuki coupling, and hinder the application of BDOPV as a building block in semiconducting polymers. So far, most of the semiconducting polymers with BDOPV adopt thiophene or its derivatives to build conjugated backbones,[30–32] and other building blocks are rarely reported, which limits the development of narrow-bandgap semiconducting polymers. Therefore, seeking a mild synthetic method and development of BDOPV-based conjugated polymers with various building blocks is important for narrow-bandgap semiconducting polymers.

[a] *School of Materials Science and Engineering, Henan University of Technology, Zhengzhou 450001, P. R. China. E-mail: tianli@haut.edu.cn*
[b] *School of Chemistry and Chemical Engineering, Henan Institute of Science and Technology, Xinxiang 453003, China*

† Electronic supplementary information (ESI) available: Additional experimental details, synthetic method, and characterization data, such as ^{1}H NMR spectra, ESR signals, and *J–V* curves, *etc*. See DOI: https://doi.org/10.1039/d3ma00073g

In this article, we have designed and synthesised a series of novel narrow-bandgap semiconducting polymers with BDOPV-based conjugated backbones (PFBP, PNBP, PBBP and PDBP) *via* a facile, fast, and highly efficient aldol condensation polymerization. The modified polymerization using triethylamine (TEA) as the catalyst requires a shorter time and milder reaction conditions. These semiconducting polymers possess an enlarged aromatic plane and high rigidity in the conjugated backbone, enabling a strong tendency of quinoid resonance which can promote the production of a red shift. Moreover, these BDOPV-based semiconducting polymers have low-lying molecular orbiters, promoting the easier n-doping behavior and stronger polaron absorption spectra. As expected, the photoelectric characteristics of these semiconducting polymers can be tuned *via* changing the copolymerization units. With the increase in the electron-withdrawing ability of the constitutional unit, the semiconducting polymers exhibit a narrower bandgap, from 1.58 eV being reduced to 1.11 eV. Then, we investigated the doping behavior with *N*-DMBI and $B(C_6F_5)_3$ (BCF) as n-type and p-type dopants, respectively. All of our semiconducting polymers can be n-doped by *N*-DMBI and especially PNBP which shows the high n-doping ability of these semiconducting polymers. Nevertheless, none of these semiconducting polymers can be p-doped by BCF, even with much more p-type dopant, which can be attributed to the shallow HOMO energy level of these near infrared polymers. This work proposes a successful design of narrow bandgap n-doped semiconducting polymers, which are thought to be a type of excellent near infrared optoelectronic materials and can provide a new design strategy and synthetic protocol for n-doped semiconducting polymers.

2. Experimental section

2.1. General synthetic method for BDOPV-based polymers

Polymers PFBP, PNBP, PBBP and PDBP were prepared by aldol condensation with triethylamine as the catalyst. Bis-isatin monomers (0.2 mmol) and bis-oxindole monomers (0.2 mml 38.0 mg) were dissolved in chlorobenzene (6 mL) followed by the addition of TEA (0.4 mmol, 56 μL) into the solution. The mixture was stirred at 70 °C for 45 min under a nitrogen atmosphere, and then *N*-methylisatin (0.6 mg, 0.004 mmol) was added as the end-capping agent. The mixture was stirred for another 10 min. After cooling to room temperature, the viscous solution was poured into anhydrous methanol and precipitated as a blue solid. The crude polymer was then re-dissolved into chloroform and precipitated from anhydrous methanol twice more, and then extracted using Soxhlet extraction successively from methanol, hexane, and chloroform and then PDBP was extra extracted by chlorobenzene. The precipitate was then collected and dried in a vacuum oven for 12 h to obtain PFBP, PNBP, PBBP and PDBP.

PFBP: M4 (0.2 mmol, 270.6 mg) and bis-oxindole monomers (0.2 mml, 38.0 mg) were used as the monomers to synthesize PFBP (235.1 mg) with a yield of 78% (M_n = 55.2 kDa).

PNBP: M6 (0.2 mmol, 323.4 mg) and bis-oxindole monomers (0.2 mml, 38.0 mg) were used as the monomers to synthesize PNBP (290.5 mg) with a yield of 82% (M_n = 20.7 kDa).

PBBP: M8 (0.2 mmol, 308.2 mg) and bis-oxindole monomers (0.2 mml, 38.0 mg) were used as the monomers to synthesize PBBP 281.4 mg) with a yield of 83% (M_n = 16.7 kDa).

PNBP: M10 (0.2 mmol, 297.4 mg) and bis-oxindole monomers (0.2 mml, 38.0 mg) were used as the monomers to synthesize PNBP (250.2 mg) with a yield of 76% (M_n = 15.9 kDa).

2.2. Characterization of monomers and polymers

The ^{1}H NMR spectra of monomers were obtained using a Bruker AVANCE Digital NMR workstation. The molecular weights of these narrow bandgap semiconducting polymers were obtained *via* a Waters GPC 2410, where high temperature chlorobenzene was chosen as the mobile phase. The UV-vis absorption spectra of these CPEs were recorded by using a HP 8453 spectrophotometer. The reduction and oxidation potentials of these polymers were recorded by electrochemical CV with a CHI660E electrochemical workstation, in a 0.1 M acetonitrile solution of tetrabutylammonium hexafluorophosphate (Bu_4NPF_6) under the protection of nitrogen. Indium tin oxide (ITO) slides coated with polymer films were used as the working electrodes, a saturated calomel electrode was chosen as the reference electrode, and a platinum wire electrode was used as the counter electrode. ESR spectroscopies of these polymers were recorded using a JEOL JES-FA200 ESR spectrometer (300 K, 9.063 GHz, Xband) at room temperature.

3. Results and discussion

3.1. Synthesis and characterization

PFBP, PNBP, PBBP and PDBP were synthesized *via* a facile, fast, and highly efficient aldol condensation polymerization, according to our previous article (experimental details and characterization

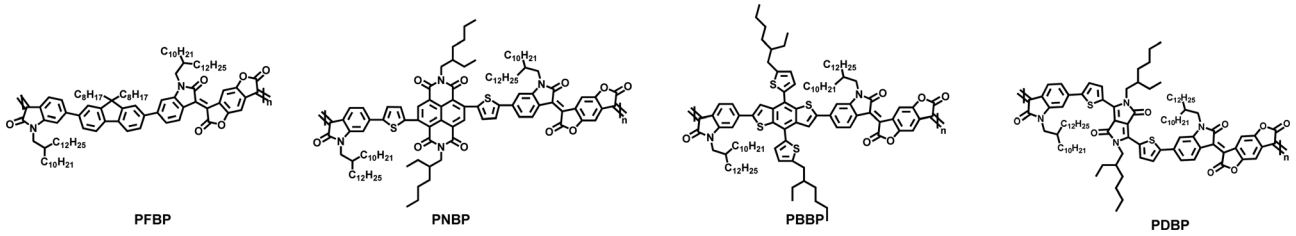

Scheme 1 Chemical structures of polymers based on BDOPV.

Table 1 Molecular weights, absorption, optical band gaps, and energy levels of PFBP, PBBP, PNBP and PDBP

Acceptor	M_n (kDa)	λ_{abs} (nm) in solution	λ_{abs} (nm) in film	E_g[a] (eV)	E_{ox} (V)	E_{re} (V)	LUMO (eV)	HOMO (eV)
PFBP	55.2	715	717	1.88	1.42	−0.46	−3.98	−5.86
PBBP	16.7	809	800	1.67	1.58	−0.42	−4.02	−5.69
PNBP	15.9	742	748	1.75	1.41	−0.34	−4.10	−5.85
PDBP	20.7	869	865	1.48	1.11	−0.37	−4.07	−5.55

[a] E_g = LUMO–HOMO.

are shown in the ESI,† Scheme S1). The chemical structures of these semiconducting polymers are shown in Scheme 1. The backbone based BDOPV unit possesses a rigid aromatic plane due to the intramolecular hydrogen bonds (Fig. S1, ESI†), resulting in reduced rotational torsion and enhanced charge transport, which facilitate the production of an intramolecular charge transport absorption peak and broaden the absorption spectrum. Furthermore, the stronger electron-withdrawing characteristic of BDOPV gives these semiconducting polymers a lower energy level and promotes chemical doping. Here, these semiconducting polymers were synthesized *via* aldol condensation polymerization with triethylamine as the catalyst. Compared with conventional aldol condensation polymerization with *p*-toluene sulfonic acid as the catalyst, the modified aldol condensation requires a shorter time and much lower temperature. Moreover, the yield of this novel aldol condensation polymerization is close to that of the conventional *p*-toluene sulfonic acid-catalyzed one.

PFBP, PNBP, and PBBP showed good solubility of over 10 mg mL^{-1} in chloroform even with the stronger rigidity in their backbones. However, PDBP with 1,4-diketopyrrolo-[3,4-*c*]-pyrroles (DPP) as the copolymerization unit showed relatively poor solubility, less than 3 mg mL^{-1} in high-temperature chlorobenzene. The number-average molecular weights (M_ns) of these polymers were obtained from gel permeation chromatography (GPC), with chlorobenzene as the mobile phases. As shown in Table 1, the M_ns of PFBP, PNBP, PBBP and PDBP are 55.2 kDa, 15.9 kDa, 16.7 kDa, and 20.7 kDa, respectively.

3.2. Optical properties

The optical absorption spectra of PFBP, PBBP, PNBP and PDBP in chloroform solution and film states are shown in Fig. 1, and the relevant parameters are summarized in Table 1. As shown in Fig. 1(a), in solution, these semiconducting polymers with different constitutional units in their backbones produced different absorption spectra on account of donor-to-acceptor ICT. The weak absorption bands from 300 nm to 500 nm of these semiconducting polymers can be attributed to characteristics of the π–π* transition in polymer backbones. And the absorption peaks located at 720 nm, 810 nm, 742 nm and 870 nm for PFBP, PBBP, PNBP and PDBP, respectively, were attributed to the ICT between the BDOPV unit and the constitutional units in the polymer backbone. In the film state (Fig. 1b), all semiconducting polymers exhibited similar absorption spectra to those in the solution state with slight red shifting, due to the increased conjugation and intermolecular interactions in the film

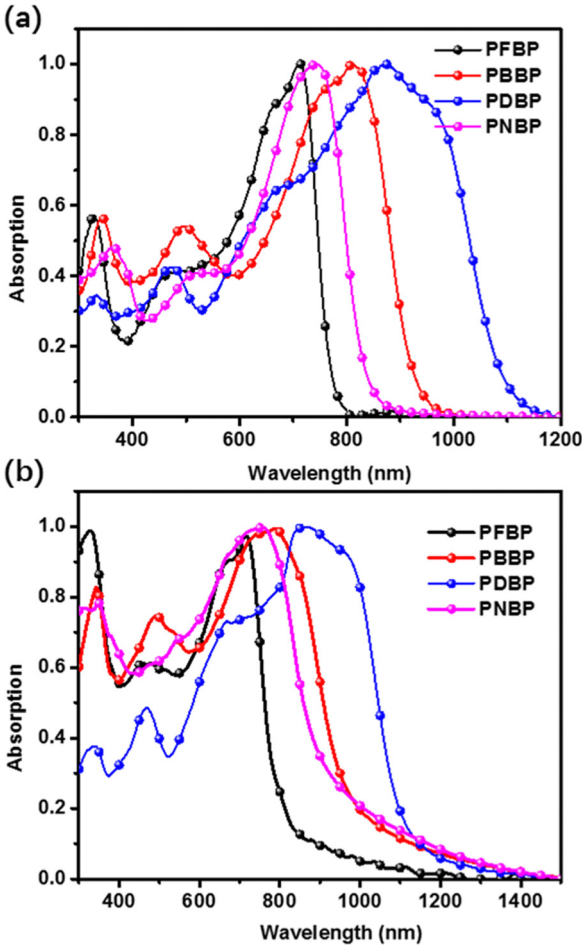

Fig. 1 The UV-vis absorption spectra of PFBP, PBBP, PNBP and PDBP (a) in chloroform and (b) in thin-film states.

state. The unexpected weakness of red shifting in the film state suggest that strong pre-aggregation occurs in solution, as a result of the high rigidity and giant "locked" aromatic plane of the conjugated backbone.[33] In these narrow-bandgap semiconducting polymers, the absorbing edge ranges from 820 nm to 1120 nm, which can be attributed to the various electron-donating/electron-withdrawing capabilities of the constitutional units. Compared with an aromatic structure, a quinoid structure usually possesses a more red-shifted absorption spectra.[34] Therefore, PDBP with a quinone steady and electron-withdrawing diketopyrrolopyrrole unit (DPP) achieves the best near infrared absorption in these semiconducting polymers, even reaching 1120 nm. The optical band gaps of PFBP, PBBP, PNBP and PDBP can be calculated from the absorption edges of their thin films, which are determined to be 1.88, 1.67, 1.75, and 1.48 eV, respectively.

3.3. Electrochemical properties

The energy levels of PFBP, PNBP, PBBP and PDBP were recorded by cyclic voltammetry (CV) analysis with a saturated calomel electrode as the reference and ferrocene/ferrocenium (Fc/Fc^+) reference as the internal standard. The CV curves of these semiconducting polymers are shown in Fig. 2, and the

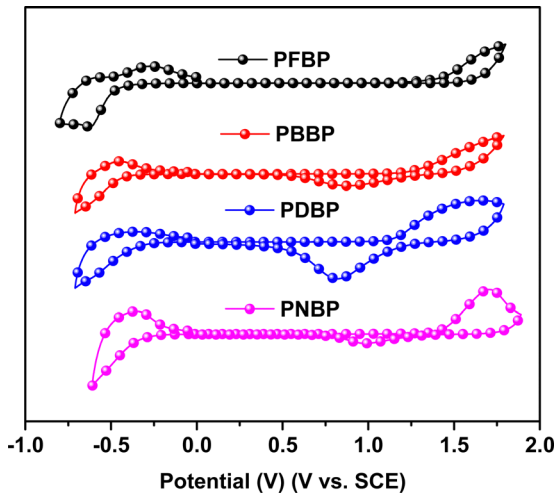

Fig. 2 The cyclic voltammetry curves of PFBP, PBBP, PNBP and PDBP.

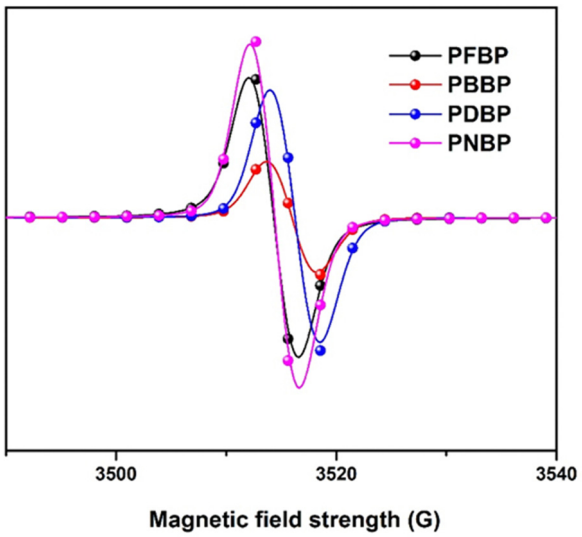

Fig. 3 The ESR signals of PFBP, PBBP, PDBP, and PNBP.

detailed electrochemical parameters are summarized in Table 1. The oxidation potentials of PFBP, PNBP, PBBP and PDBP were estimated to be 1.42, 1.41, 1.58 and 1.11 V, respectively. And the highest occupied molecular orbital energy level (HOMO) energy levels of these semiconducting polymers were calculated to be −5.86, −5.85, −5.69 and −5.55 eV, respectively. The reduction potentials of the PFBP, PNBP, PBBP and PDBP polymers were −0.46, −0.34 and −0.37 V, respectively, corresponding to the lowest unoccupied molecular orbital energy levels (LUMO) of −3.98, −4.10, −4.02 and −4.07 eV, respectively. The HOMO energy levels of these semiconducting polymers are fluctuated as variant electron-donating/electron-withdrawing capability of the constitutional units. However, all of these semiconducting polymers exhibit similar LUMO levels, and the low-lying LUMO levels of these semiconducting polymers are favorable for the occurrence of n-type doping,[35] which can promote the production of a polaron and broaden the absorption spectrum.

3.4. Electron spin resonance spectroscopy

In order to explore the quinoid resonance of these narrow-bandgap semiconducting polymers in the solid state, electron spin resonance (ESR) spectroscopy was conducted, and the results are shown in Fig. 3. Equal amounts of each solid state semiconducting polymer were submitted for the test under an atmospheric environment. All polymers exhibited ESR signal intensities with slightly different field strengths because of the various conjugated backbones. These polymers presented obvious ESR signals, which can originate in the induced diradicals for the quinoid structure. This result indicates that these BDOPV-based semiconducting polymers tend to occur with quinoid resonance in the solid state,[36,37] which can narrow the bandgaps.

3.5. Charge transport properties

The electron/hole mobility of these narrow-bandgap semiconducting polymers was investigated using electron-only devices with indium tin oxide (ITO)/ZnO/polymers/Ag structures and hole-only devices with ITO/PEDOT:PSS/polymers/MoO_3/Ag structures, respectively. A space charge limited current (SCLC) model was applied to calculate the electron/hole mobilities of these polymers. Fig. 4 shows the *J*–*V* curves of these semiconducting polymers, and Table S1 (ESI†) summarizes the corresponding electron/hole mobility values. Interestingly, these BDOPV-based semiconducting polymers with different constitutional units present various charge transfer characteristics. Notably, PFBP exhibits a typical n-type semiconductor characteristic, whose electron mobility is two orders of magnitude larger than the hole mobility values. PNBP and PDBP possess comparable electron mobilities and hole mobilities, and exhibit amphoteric semiconductor characteristics. PBBP with a hole mobility two orders larger than the electron mobility can even be considered as a p-type semiconductor, to a certain extent. This result indicates that the electrical properties of constitutional units could strongly influence the charge transporting properties and semiconductor characteristics of BDOPV-based semiconducting polymers. X-ray diffraction was carried out to research the molecular packing structure of all the polymers. They all showed similar spectra, indicating similar molecular packing structures (Fig. S2, ESI†). We also tried to evaluate the conductivity of these CPEs *via* a four-probe method. The conductivity of PFBP, PBBP, PNBP, and PDBP was estimated to be $(3.10 \pm 1.02) \times 10^{-4}$, $(4.26 \pm 1.17) \times 10^{-4}$, $(3.27 \pm 1.40) \times 10^{-4}$, and $(6.55 \pm 0.37) \times 10^{-4}$ S cm^{-1}, respectively.

3.6. Photovoltaic performance

These narrow-bandgap semiconducting polymers with a red-shift absorption spectrum and a low LUMO energy level have potential applications in all polymer solar cells (All-PSCs). We tried to investigate the photovoltaic performance of these semiconducting polymers, and all the polymers except for PDBP were applied as polymer acceptors with PTB7-Th in All-PSCs, due to the low solubility of PDBP. All-PSC devices with an architecture of ITO/PEDOT:PSS/PBDB-T:acceptor/PFN-Br/Ag

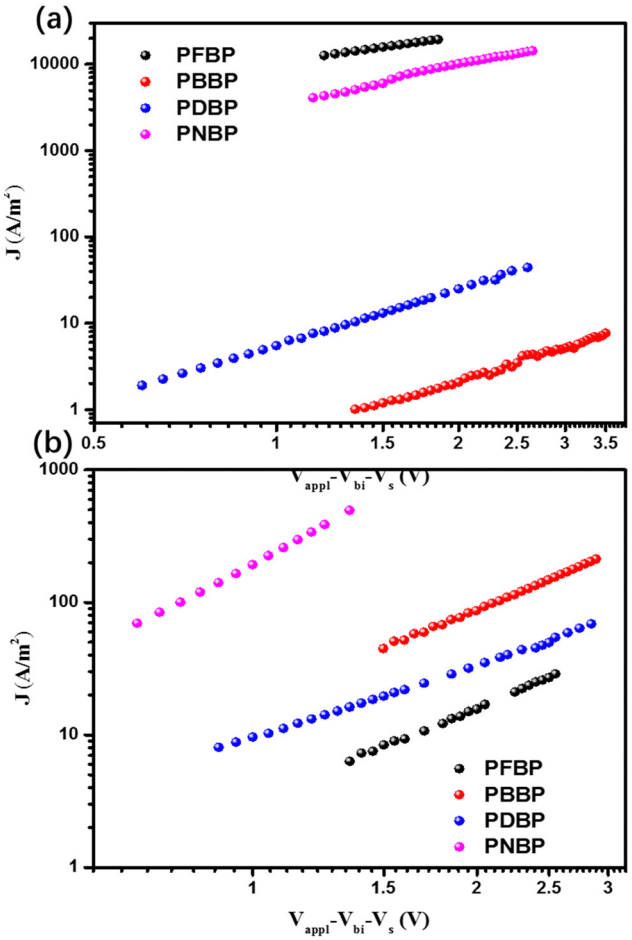

Fig. 4 The *J*–*V* curves of (a) electron-only devices with the structure ITO/ZnO/polymers/Ag; (b) hole-only devices with the structure ITO/PEDOT:PSS/polymers/MoO_3/Ag for semiconducting polymer films.

were fabricated. Disappointingly, All-PSC with PFBP, PBBP and PNBP as the acceptors produce poor power conversion efficiencies (PCE), less than 0.2%. The *J*–*V* characteristics are shown in Fig. S3 (ESI†) and the device parameters are summarized in Table S2 (ESI†).

The UV-Vis absorption spectra and the photoluminescence (PL) spectra (excitation wavelength at 680 nm) of the polymer:PTB7-Th blend films were recorded to test the charge transfer between the polymer and PTB7-Th. As shown in Fig. S4b (ESI†), there is a visible PL peak at 755 nm for the pure PTB7-Th film. However, in the PL spectra of the polymer: PTB7-Th blend films, the PL peaks at 755 nm disappeared. This result indicates that there exists an efficient charge transfer between these polymers and PTB7-Th. This could be due to the matched LUMO levels of semiconducting polymers with that of PTB7-Th.

In order to further investigate the reason for the inferior performance of these All-PSCs, we then fabricated electron-only devices and hole-only devices with a polymer: PTB7-Th blend film to explore the charge transport properties of the active layer, and the corresponding *J*–*V* curves are shown in Fig. S5 (ESI†), and the electron/hole mobilities are summarized in Table S1 (ESI†). From Table S4 (ESI†), it can be found that the hole mobilities of these blend films are three or four orders of magnitude higher than their electron mobilities. These extremely unbalanced electron/hole mobilities will lead to an imbalance of extraction, and affect the fill factor (FF) and short-circuit current (J_{sc}).

3.7. Doping properties

In order to explore the doping behavior of these narrow-bandgap semiconducting polymers, UV-vis absorption spectroscopy of PFBP, PNBP, PBBP and PDBP in chloroform solution with *N*-DMBI and BCF (Fig. 5) as the n-type and p-type dopants was carried out. As shown in Fig. 6, a small amount of *N*-DMBI (0.5 wt% for semiconducting polymers) can largely trigger the formation of new polaron absorption bands (from 1000 nm to 1200 nm) in the spectra of these polymers except PDBP. For PDBP an obvious red-shift is observed in the absorption spectra, due to the overlap of the character peaks for charge transfer and polaron absorption bands. These results indicate that all of these narrow-bandgap semiconducting polymers are easily n-doped. This phenomenon might be attributed to the giant "locked" aromatic plane of the BDOPV unit in the backbone arising from the hydrogen bonds between the phenyl protons and neighboring carbonyl group in BDOPV, resulting in good planarity and shape-persistency for the conjugated backbone, which eliminates the rotational torsion and is advantageous to interchain electronic coupling and charge transport. Besides, the strong electron-withdrawing BDOPV unit can decrease the LUMO energy of the conjugated backbone, which may promote the n-doping behavior of these polymers. However, as for the p-type dopant, the absorption spectra of these polymers with the same amount (0.5 wt% for semiconducting polymers) of BCF are similar to those of the pure polymers (Fig. 1). Further enhancing the equivalent of BCF to 200 wt% for semiconducting polymers, the polaron absorption still cannot be observed in the absorption spectra of these narrow-bandgap polymers. Then in order to further test the p-doping ability of these polymers, the absorption spectra of the narrow-bandgap polymers in the film state with BCF (200 wt%) were researched. As shown in Fig. S6 (ESI†), after thermal annealing at 120 °C for different amounts of time, there is negligible difference in the absorption spectra of these polymers, which indicates that these semiconducting polymers can rarely be doped by BCF. The shallow HOMO energy level of those semiconducting

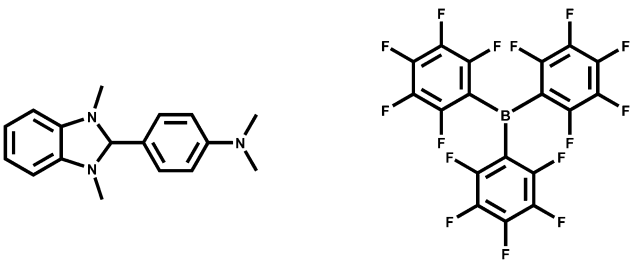

Fig. 5 Chemical structures of *N*-DMBI and BCF.

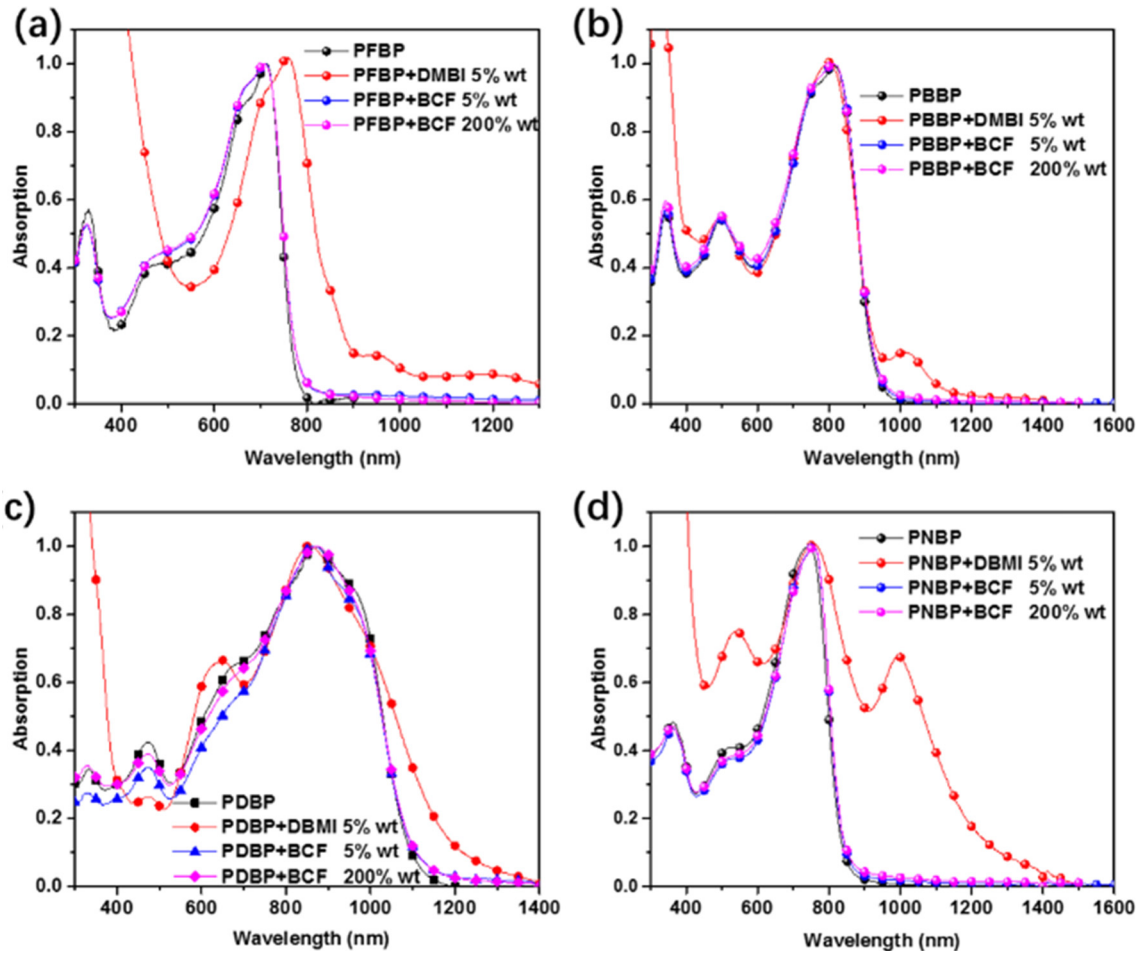

Fig. 6 UV-vis absorption spectra of PFBP (a), PBBP (b), PDBP (c), and PNBP (d) with *N*-DMBI and BCF as the n-type and p-type dopants.

polymers which is near or even higher than the doping limit of BCF (5.8 eV) should account for the extremely poor p-doping behavior with BCF.

4. Conclusions

In summary, a modified aldol condensation protocol with mild reaction conditions and high efficiency was used to synthesize a series of low bandgap semiconducting polymers with BDOPV-based conjugated backbones. These BDOPV-based polymers showed a better molecular plane, conjugate effect and tendency of quinoid resonance due to the intramolecular hydrogen bonding, resulting in near infrared absorption. Moreover, the semiconductor properties of these polymers can be tuned *via* the various constitutional units, from an n-type character switched into an ambipolar and even p-type character. In addition, these BDOPV-based low bandgap polymers with *N*-DMBI as additional n-type dopants exhibit obvious polaron absorption, indicating the better n-doped ability of these polymers. Finally, All-PSCs with these polymers as the acceptor were prepared and achieved poor efficiency, due to the extremely unbalanced electron/hole mobilities. These results indicate that BDOPV-based semiconducting polymers are a class of promising narrow-bandgap semiconducting polymers that possess an excellent n-doping ability.

Conflicts of interest

The authors declare no conflicts of interest.

Acknowledgements

This work was financially supported by the Science Foundation of Henan University of Technology (grant no. 2021BS044) and The Open Fund for Key Lab of Guangdong High Property and Functional Macromolecular Materials, China (20220608).

References

1 P. C. Y. Chow and T. Someya, *Adv. Mater.*, 2020, **32**, 1902045.
2 Y. Huang, C. Jiang, Y. Zhu, S. Zhang, G. Li, Z. Yao, C. Li, X. Wan and Y. Chen, *Org. Electron.*, 2022, **110**, 106642.
3 J. Yee Low, Z. Merican Aljunid Merican and M. Falalu Hamza, *Mater. Today Proc.*, 2019, **16**, 1909–1918.
4 J. Liang, L. Ying, F. Huang and Y. Cao, *J. Mater. Chem. C*, 2016, **4**, 10993–11006.

5 G. Wang, F. S. Melkonyan, A. Facchetti and T. J. Marks, *Angew. Chem., Int. Ed.*, 2019, **58**, 4129–4142.
6 Z.-G. Zhang and Y. Li, *Angew. Chem., Int. Ed.*, 2021, **60**, 4422–4433.
7 D.-T. Nguyen, S. Sharma, S.-A. Chen, P. V. Komarov, V. A. Ivanov and A. R. Khokhlov, *Mater. Adv.*, 2021, **2**, 1016–1023.
8 C. Cui and Y. Li, *Energy Environ. Sci.*, 2019, **12**, 3225–3246.
9 H. Sun, X. Guo and A. Facchetti, *Chem*, 2020, **6**, 1310–1326.
10 L. Li, L. Han, H. Hu and R. Zhang, *Mater. Adv.*, 2023, **4**, 726–746.
11 J. Qin, L. Zhang, C. Zuo, Z. Xiao, Y. Yuan, S. Yang, F. Hao, M. Cheng, K. Sun, Q. Bao, Z. Bin, Z. Jin and L. Ding, *J. Semicond.*, 2021, **42**, 010501.
12 J. Yang, N. An, S. Sun, X. Sun, M. Nakano, K. Takimiya, B. Xiao and E. Zhou, *Sci. China: Chem.*, 2019, **62**, 1649–1655.
13 S. Griggs, A. Marks, H. Bristow and I. McCulloch, *J. Mater. Chem. C*, 2021, **9**, 8099–8128.
14 D. Liu, D. Yang, Y. Gao, J. Ma, R. Long, C. Wang and Y. Xiong, *Angew. Chem., Int. Ed.*, 2016, **55**, 4577.
15 J. Lee, H. Cha, H. Yao, J. Hou, Y.-H. Suh, S. Jeong, K. Lee and J. R. Durrant, *ACS Appl. Mater. Interfaces*, 2020, **12**, 32764–32770.
16 J. Lee, S. Song, J. Huang, Z. Du, H. Lee, Z. Zhu, S.-J. Ko, T.-Q. Nguyen, J. Y. Kim, K. Cho and G. C. Bazan, *ACS Mater. Lett.*, 2020, **2**, 395.
17 C. He, Y. Li, Y. Liu, Y. Li, G. Zhou, S. Li, H. Zhu, X. Lu, F. Zhang, C.-Z. Li and H. Chen, *J. Mater. Chem. A*, 2020, **8**, 18154.
18 C.-K. Wang, B.-H. Jiang, J.-H. Lu, M.-T. Cheng, R.-J. Jeng, Y.-W. Lu, C.-P. Chen and K.-T. Wong, *ChemSusChem*, 2020, **13**, 903.
19 Y. Chen, Y. Zheng, Y. Jiang, H. Fan and X. Zhu, *J. Am. Chem. Soc.*, 2021, **143**, 4281–4289.
20 T. Han, Z. Wang, N. Shen, Z. Zhou, X. Hou, S. Ding, C. Jiang, X. Huang, X. Zhang and L. Liu, *Nat. Commun.*, 2022, **13**, 1332.
21 T. Wang, R. Sun, X.-R. Yang, Y. Wu, W. Wang, Q. Li, C.-F. Zhang and J. Min, *Chin. J. Polym. Sci.*, 2022, **40**, 877–888.
22 C. Mu, P. Liu, W. Ma, K. Jiang, J. Zhao, K. Zhang, Z. Chen, Z. Wei, Y. Yi, J. Wang, S. Yang, F. Huang, A. Facchetti, H. Ade and H. Yan, *Adv. Mater.*, 2014, **26**, 7224–7230.
23 G. P. Kini, J. Y. Choi, S. J. Jeon, I. S. Suh and D. K. Moon, *Polym. Chem.*, 2019, **10**, 4459–4468.
24 K. Shi, F. Zhang, C.-A. Di, T.-W. Yan, Y. Zou, X. Zhou, D. Zhu, J.-Y. Wang and J. Pei, *J. Am. Chem. Soc.*, 2015, **137**, 6979–6982.
25 J. Yao, B. Qiu, Z.-G. Zhang, L. Xue, R. Wang, C. Zhang, S. Chen, Q. Zhou, C. Sun, C. Yang, M. Xiao, L. Meng and Y. Li, *Nat. Commun.*, 2020, **11**, 2726.
26 M. Lv, Y. Li, X. Wei, Y. Xu, Z. Ge and X. Chen, *ACS Appl. Energy Mater.*, 2019, **2**, 2238–2245.
27 R. Yamachika, M. Grobis, A. Wachowiak and M. F. Crommie, *Science*, 2004, **304**, 281–284.
28 R. A. Schlitz, F. G. Brunetti, A. M. Glaudell, P. L. Miller, M. A. Brady, C. J. Takacs, C. J. Hawker and M. L. Chabinyc, *Adv. Mater.*, 2014, **26**, 2825–2830.
29 C. G. Tang, M. N. Syafiqah, Q.-M. Koh, C. Zhao, J. Zaini, Q.-J. Seah, M. J. Cass, M. J. Humphries, I. Grizzi, J. H. Burroughes, R.-Q. Png, L.-L. Chua and P. K. H. Ho, *Nature*, 2019, **573**, 519–525.
30 T. Lei, J.-H. Dou, X.-Y. Cao, J.-Y. Wang and J. Pei, *Adv. Mater.*, 2013, **25**, 6589–6593.
31 Z.-F. Yao, Y.-Q. Zheng, Q.-Y. Li, T. Lei, S. Zhang, L. Zou, H.-Y. Liu, J.-H. Dou, Y. Lu, J.-Y. Wang, X. Gu and J. Pei, *Adv. Mater.*, 2019, **31**, 1806747.
32 Z.-F. Yao, H.-Y. Liu, Z.-Y. Wang, Z.-K. Zhou, J.-Y. Wang and J. Pei, *Chem. – Asian J.*, 2019, **14**, 1686.
33 P. J. Brown, D. S. Thomas, A. Köhler, J. S. Wilson, J.-S. Kim, C. M. Ramsdale, H. Sirringhaus and R. H. Friend, *Phys. Rev. B: Condens. Matter Mater. Phys.*, 2003, **67**, 064203.
34 M. R. Rao, S. Johnson and D. F. Perepichka, *Org. Lett.*, 2016, **18**, 3574–3577.
35 S. Guha, F. S. Goodson, L. J. Corson and S. Saha, *J. Am. Chem. Soc.*, 2012, **134**, 13679–13691.
36 Y. Li, L. Li, Y. Wu and Y. Li, *J. Phys. Chem. C*, 2017, **121**, 8579–8588.
37 D. Huang, H. Yao, Y. Cui, Y. Zou, F. Zhang, C. Wang, H. Shen, W. Jin, J. Zhu, Y. Diao, W. Xu, C.-A. Di and D. Zhu, *J. Am. Chem. Soc.*, 2017, **139**, 13013.